FIBULA SMRA 20-19066-10 - BRASS - ROMAN TIMES - SWITZERLAND

Artefact name Fibula SMRA 20-19066-10

Authors Christian. Degrigny (HE-Arc CR, Neuchâtel, Neuchâtel, Switzerland) & Naima. Gutknecht (HE-Arc CR, Neuchâtel, Neuchâtel, Switzerland) & Valentina. Valbi (Laboratoire Métallurgie et Culture LMC-IRAMAT-CNRS-UTBM, Belfort, Franche-Comté, France)

Url /artefacts/1323/

The object

Credit SMRA.

Fig. 1: Fibula (side A),

Description and visual observation

Description of the artefact	Fibula with an outwardly curved hinge, a profiled arch decorated with a succession of narrow, grooved and toric mouldings and a smooth triangular foot finished with two small mouldings. Typology Riha 5.6. Brown appearance with residues of a shiny metallic grey coating on the arch. The surface is flaking on the pin. Residue of soil sediment on the arch. L = 48mm. W = 4.7g.
Type of artefact	Jewellery
Origin	Avenches, Switzerland, Avenches, Vaud, Switzerland
Recovering date	2020
Chronology category	Roman Times
chronology tpq	----
chronology taq	----
Chronology comment	
Burial conditions / environment	Soil
Artefact location	Site et musée romains Avenches, Avenches, Vaud
Owner	Site et musée romains Avenches, Avenches, Vaud
Inv. number	SMRA 20/19066-10
Recorded conservation data	Partially cleaned with ethanol and a soft brush.

Complementary information

The fibula was found at village ***Derrière les murs***, near Avenches.

Study area(s)

Credit SMRA/HE-Arc CR_N.Gutknecht.

Fig. 2: Location of XRF analyses (red circles), Fig. 3 (documentation of corrosion structure (blue square)) and sampling for cross-section,

Binocular observation and representation of the corrosion structure

The schematic representation below gives an overview of the corrosion structure encountered on the pin of the fibula from a first visual macroscopic observation.

Strata	Type of strata	Principal characteristics
S1	Soil	crust, light brown, thin, discontinuous, matte, non compact, friable, very soft
CP1	Corrosion product	layer, olive green, thin, discontinuous, submetallic, compact, brittle, soft
CP2	Corrosion product	layer, brown, thin, discontinuous, matte, compact, brittle, very soft
CP3	Corrosion product	layer, olive green, thick, discontinuous, matte, compact, brittle, soft
CP4	Corrosion product	layer, dark brown, thin, discontinuous, matte, compact, brittle, soft
CP5	Corrosion product	layer, light green, thin, discontinuous, matte, non compact, powdery, very soft
CP6	Corrosion product	layer, dark green, thin, continuous, matte, non compact, friable, very soft
CP7	Corrosion product	layer, olive green, thin, continuous, matte, non compact, powdery, very soft
M1	Metal	layer, dark yellow, metallic, thick, continuous, compact, tough

Table 1: Description of the principal characteristics of the strata as observed under binocular and described according to Bertholon's method.

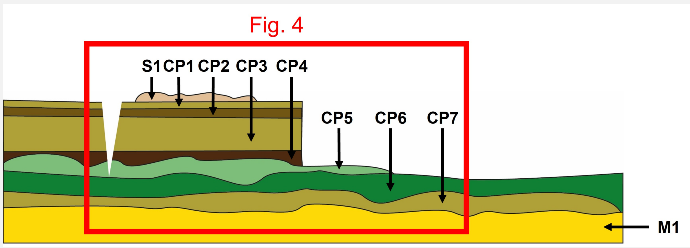

Credit HE-Arc CR, N.Gutknecht.

Fig. 3: Stratigraphic representation of the corrosion structure on the fibula by macroscopic and binocular observation with location of Fig. 4,

MiCorr stratigraphy(ies) – Bi

Fig. 4: Stratigraphic representation observed macroscopically under binocular using the MiCorr application with reference to Fig. 3. The characteristics of the strata are only accessible by clicking on the drawing that redirects you to the search tool by stratigraphy representation, Credit HE-Arc CR, N.Gutknecht.

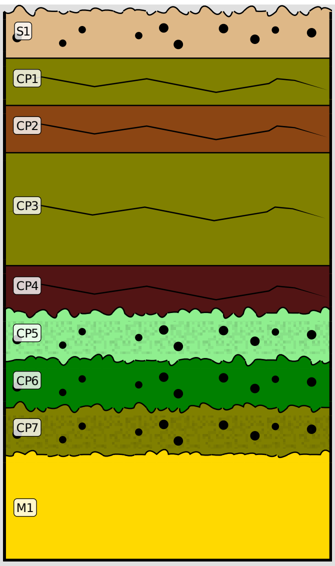

Sample(s)

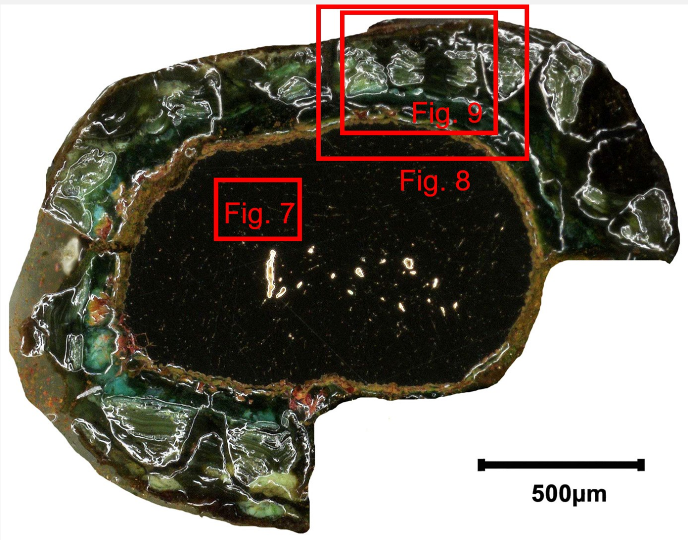

Credit LMC-CNRS, V.Valbi.

Fig. 5: Micrograph of the cross-section of the sample from Fig. 2 in dark field showing the location of Figs. 7-9,

Description of sample	The cross-section corresponds to a lateral cut (Fig. 2). The sample was cut from the central body of the pin after embedding one part of the object in the resin. A metal core is still present under the corrosion layers (Fig. 5).
Alloy	Brass
Technology	Annealed after cold working
Lab number of sample	SMRA_fibule
Sample location	Site et musée romains Avenches, Avenches, Vaud
Responsible institution	Site et musée romains Avenches, Avenches, Vaud
Date and aim of sampling	January 2021

Complementary information

Sample taken from the object is embedded in resin and kept by the institution with the object if further analysis is needed.

Analyses and results

Analysis performed :

Non-Invasive approach

- XRF with handheld portable X-ray fluorescence spectrometer (NITON XL3t 950 Air GOLDD+, Thermo Fischer®). General Metal mode, acquisition time 60s (filters: Li20/Lo20/M20).

Invasive approach (on the sample)

- Optical microscopy: the sample is polished, then it is observed using a digital microscope KEYENCE VHX-7000 in bright and dark field.
- Metallography: the polished sample is etched with alcoholic ferric chloride and observed by optical microscopy in bright field.
- SEM-EDS: the sample is coated with a carbon layer and analysis are performed on a SEM-FEG JEOL 7001-F equipped with a silicon-drift EDS Oxford detector (Aztec analysis software) with an accelerating voltage of 20 kV and probe current at about 9 nA. The relative error is considered of about 10% for content range <1wt%, and 2% for content range of >1wt%.
- µ-Raman spectroscopy: it is performed on a HORIBA Labram Xplora spectrometer equipped with a 532 nm laser with 1800 grating, the laser power employed is between 0.04 and 0.55 mW with acquisition time varying between 1 and 5 minutes.

Non invasive analysis

XRF analyses were carried out on the surface of the object (Fig. 2). All strata (soil, corrosion products and metal) are analyzed at the same time. While the pin (point 1) is showing little sediments and a clear delimitation of the original surface with loss of the internal corrosion layers, the arch (point 2) has a thick layer of soil and external corrosion. The metal on the pin is presumably a copper-based alloy with high contents of Zn and Sn. The metal of the arch has a higher amount of Sn and shows the presence of lead. This could be due to the presence of decorative incrustation, surface tinning or a surface enrichment on the arch. Si, Fe, Al, S and P detected are probably coming from the burial environment.

Element (mass %)	1	σ	2	σ
Cu	80.9	0.54	33.6	0.12
Sn	7.5	0.1	26.8	0.12
Zn	7.7	0.09	2.1	0.03
Pb	0.2	0.02	12.5	0.06
Si	2.4	0.25	9.72	0.14
Fe	0.3	0.02	8.9	0.08
Al	n.d.	n.d.	3.4	0.19
S	0.3	0.06	n.d.	n.d.
P	0.4	0.08	2.2	0.05
Sb	0.16	0.02	0.2	0.01

Table 2: Chemical composition of the surface of the fibula at two representative points shown in Fig. 2 (n.d.: below the detection limit), HE-Arc CR.

Metal

EDX analysis (Table 3) of the residual metal of the pin on cross-section shows that it is a Cu-Zn-Sn brass alloy with a medium amount of Zn (13 wt%) and 3 wt% of Sn. The results obtained are in agreement with the non-invasive XRF analysis (see table 2, point 1).

The observation of the metal in cross-section after etching (Fig. 6) shows a microstructure with polygonal grains and several twinned grains (Fig. 7), revealing that the object underwent cold working and annealing. The metal presents porosities and sulfide inclusions (Fig. 7) for a total of 1% of the metallic surface of the sample in cross-section.

Elements	wt %
Cu	83
Zn	13
Sn	3
Na	<0.5
Al	<0.5
S	<0.5
Fe	<0.5

Table 3: Chemical composition (wt %) of the alloy over a general area of analysis obtained by SEM-EDX, LMC-IRAMAT-CNRS-UTBM.

Fig. 6: Micrograph of the cross-section of the sample (same as Fig. 5) in bright field after chemical etching,

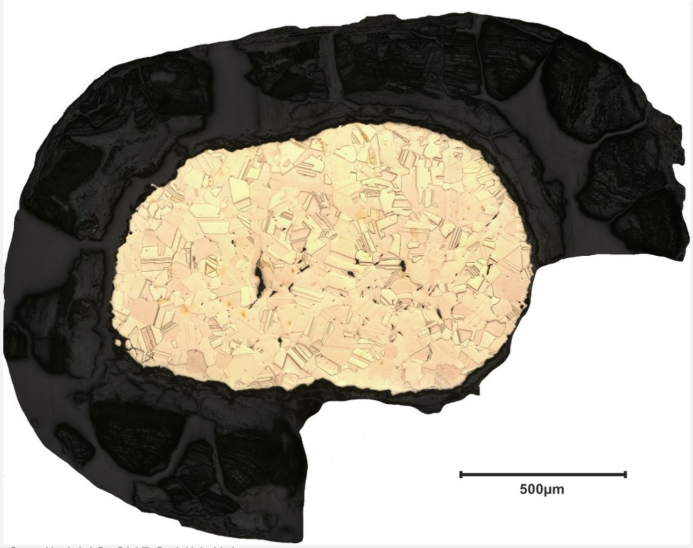

Credit LMC-CNRS, V.Valbi.

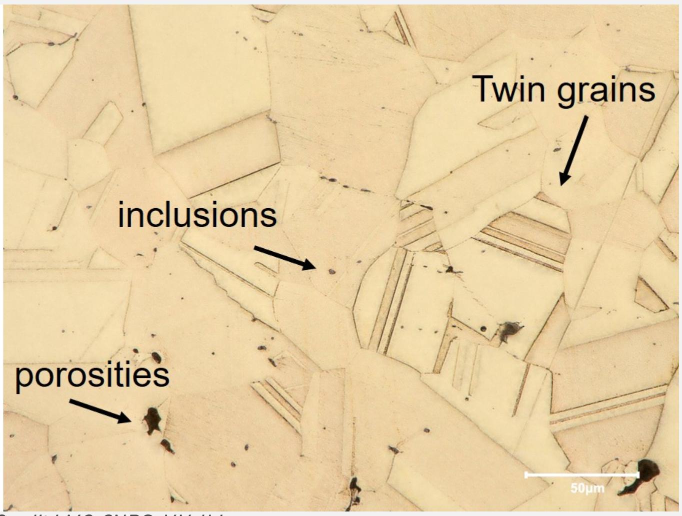

Credit LMC-CNRS, V.Valbi.

Fig. 7: Micrograph of the metal sample from Fig. 6 (detail), etched, bright field. A polygonal grain microstructure is observed, with the presence of twin grains, inclusions and porosities,

Microstructure	Polygonal and twinned grains
First metal element	Cu
Other metal elements	Zn, Sn

Complementary information

None.

Corrosion layers

The observation of the sample in cross-section in dark field (Fig. 8) allows to identify an external sediment soil (S1), a thin (5 *µm)* dark brown CP1, a thick (200 *µm)* foliated (alternative bands) green stratum (CP2), a dark green stratum 100 *µm thick* (CP3), a red 30 *µm thin* stratum (CP4) and M1.

The SEM-EDX analyses (Table 4, Fig. 9) and Raman spectroscopy (Fig. 10) allow to identifiy the CP4 as cuprite (Cu_2O) while the other strata present too much fluorescence to be identified by Raman spectroscopy. The SEM-EDX shows that all the corrosion structure is depleted in Zn and enriched in Sn, especially the CP1 (Sn 41 wt%). CP1 and CP2 are also enriched in Fe, P and Ca from the soil. The S1 stratum presents an enrichment in Sn and O, as well as external elements such as Ca and Fe. It corresponds to the Transformed Medium (Neff et al. 2004), a transition zone between the Dense Product Layer (DPL) and the non altered soil, containing both corrosion products and markers from the soil. No significant Cl enrichment is observed.

wt%	S1	CP1	CP2	CP3	CP4
O	33	20	28	33	12
Cu	12	17	33	30	79
Sn	34	41	27	30	6
Zn	2	1	<0.5	1	1

Fe	7	11	5	1	n.d.
Si	1	3	3	2	<0.5
P	1	2	1	<0.5	<0.5
Ca	6	3	2	1	<0.5
Pb	1	1	1	<0.5	<0.5
Al	<0.5	1	<0.5	n.d.	n.d.
S	1	<0.5	<0.5	<0.5	n.d.
Cl	1	<0.5	<0.5	1	1

Table 4: Chemical composition (wt%) of the corrosion products over a general area of analysis by SEM-EDX (n.d.: below the detection limit), LMC-IRAMAT-CNRS-UTBM.

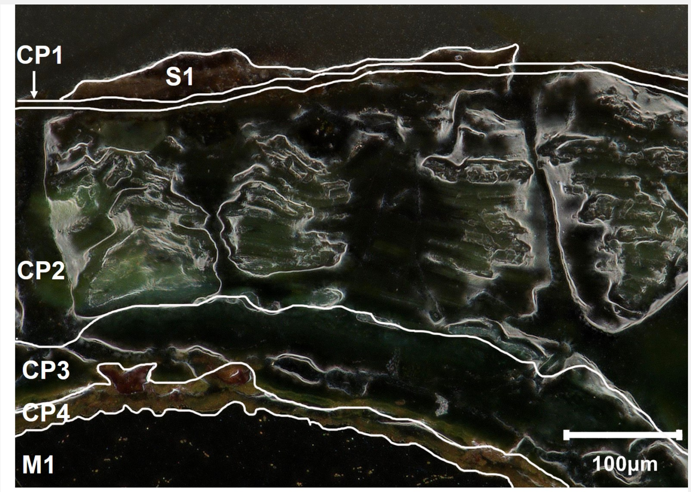

Credit LMC-CNRS, V.Valbi.

Fig. 8: Micrograph of the corrosion structure of the sample from Fig. 5 (detail), unetched, dark field. The strata S1 to M1 are indicated and also shown in the digital stratigraphy in Fig. 11,

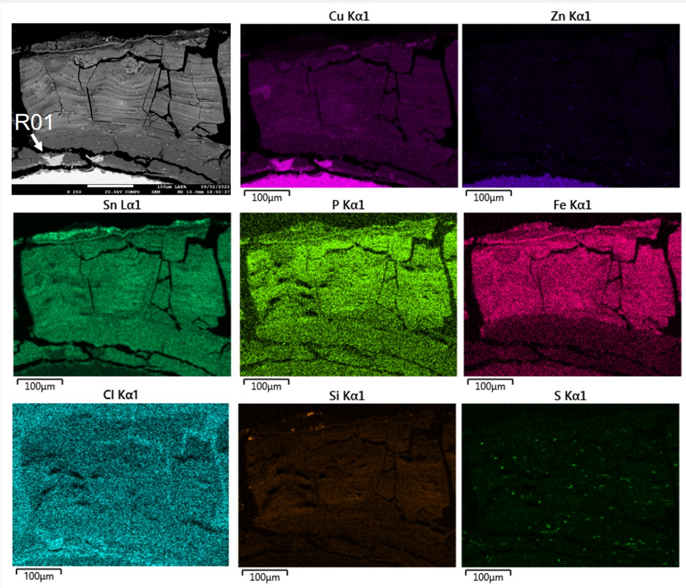

Credit LMC-CNRS, V.Valbi.

Fig. 9: SEM image, BSE-mode, and elemental chemical distribution of the selected area. The selected point for Raman analysis shown in Fig. 10 is indicated,

Fig. 10: Raman spectrum of point R01 (together with the RRUFF reference RRUFFID=R140763 for cuprite) showed in Fig. 9,

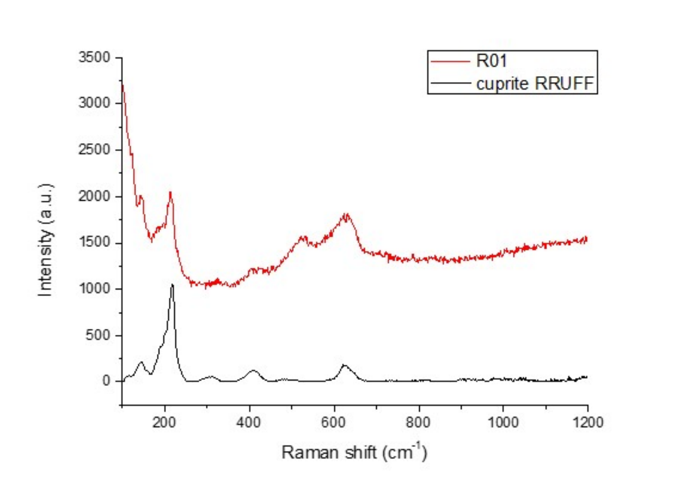

Credit LMC-CNRS, V.Valbi.

Corrosion form	Uniform
Corrosion type	Unknown

Complementary information

None.

MiCorr stratigraphy(ies) – CS

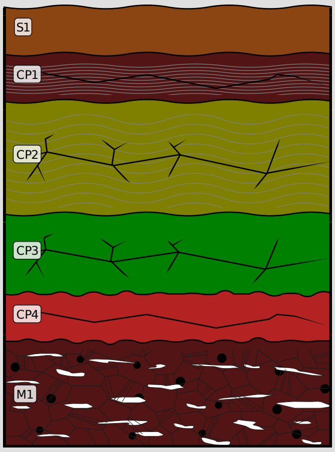

Fig. 11: Stratigraphic representation of the sample from the roman fibula in cross-section (dark field) using the MiCorr application. The characteristics of the strata are only accessible by clicking on the drawing that redirects you to the search tool by stratigraphy representation. This representation was build according to Fig. 8, Credit LMC-CNRS, V.Valbi.

Synthesis of the binocular / cross-section examination of the corrosion structure

The observation under binocular microscope identified 7 CPs while the cross-section identified 4 CPs.

With binocular microscope, it is possible to differentiate strata according to texture and light color changes that do not always correspond to significative changes in chemical composition, thus leading to a regrouping of several strata into one in the cross-section observation and physicochemical characterization. The differences between the two observation modes could also be explained by different locations of observation.

Both observation modes identified one S1 stratum. The CP1 and CP2 under binocular microscope could be grouped and correspond to CP1 in CS. Similarly, the CP3 and CP4 under binocular probably correspond to CP2 in cross-section; the CP5 and CP6 under binocular could correspond to CP3 in cross-section. CP7 under binocular and CP4 in cross-section could not be linked as their characteristics are so different.

Fig. 12: Stratigraphic representation side by side of binocular view and cross-section (dark field),

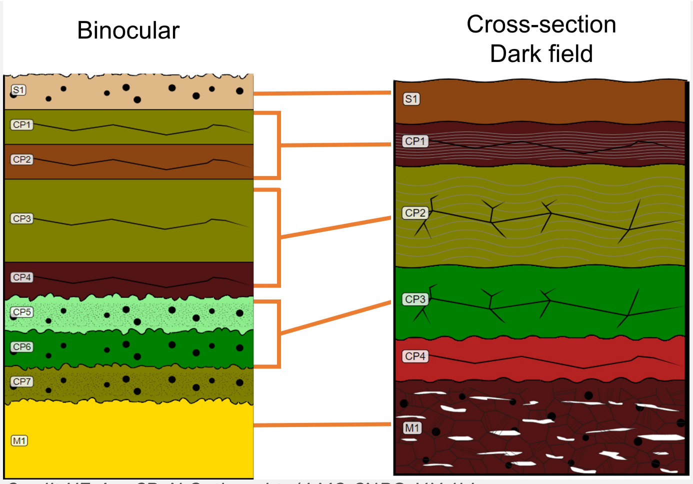

Credit HE-Arc CR, N.Gutknecht, / LMC-CNRS, V.Valbi.

Conclusion

The fibula is a brass with a a medium amount of Zn (13 wt%) and low amount of Sn (3 wt%). The microstructure of the metal shows that it underwent cold working and annealing.

After observation of the corrosion structure in cross-section, it is possible to identify the original surface of the object that has been preserved and corresponds to the interface between CP1 and S1. As for the corrosion structure underneath, it presents the phenomenon of dezincification commonly observed in brasses, together with a decuprification phenomenon. In fact Zn is almost absent in the whole corrosion structure (1 mass%), Cu is strongly depleted (20-30 mass%) while a strong enrichment in Sn is observed (30-40 wt%). A strong fluorescence signal in Raman did not allow to clearly identify the compounds constituting CP2 and CP3, while CP4 was identified as copper oxide cuprite. However, EDX analysis indicates that CP2 shows a strong enrichment in soil elements (Fe, P), associated with a foliated and cracked morphology that could favor the penetration of these external elements.

This artefact is part of a corpus of objects, together with Earstick SMRA 20/19047-03 and Ring SMRA 16/17285-01 which all present a flaking phenomenon of the corrosion products.

References

References on object and sample

1. Earstick SMRA 20/19047-03
2. Ring SMRA 16/17285-01

References on analytical methods and interpretation

3. Lafuente, B., Downs, R. T., Yang, H., Stone, N. (2015) The power of databases: the RRUFF project. In: Highlights in Mineralogical Crystallography, T. Armbruster and R. M. Danisi, eds. Berlin, Germany, W. De Gruyter, 1-30.
4. Papadopoulou, O., Vassiliou, P., Grassini, S., Angelini, E. and Gouda, V. (2016) Soil-induced corrosion of ancient Roman brass – A case study. Materials and Corrosion, 67, 2.5. Scott, D. (2006) Metallography and microstructure of ancient and historic metals. J Paul Getty Museum Publications.
6. Robbiola L., Blengino M., Fiaud C., (1998) Morphology and mechanisms of formation of natural patinas on archaeological Cu–Sn alloys. Corrosion Science, 40 (12), 2083-2111.
7. Neff D., Reguer S., Bellot-Gurlet L., Dillmann P., Bertholon R. (2004) Structural characterization of corrosion products on archaeological iron: an integrated analytical approach to establish corrosion forms. J. Raman Spectrosc. 35: 739–745.